Current Blockage in Steady Flow: Interaction of Uniform and Sheared Flow with a Porous Body having Uniform and Non-uniform Resistance

H. Santo[1], P. H. Taylor[1,2,3] and S. Draper[3]

[1]1Department of Civil and Environmental Engineering, National University of Singapore, 117576, Singapore

[2]Department of Engineering Science, University of Oxford, Oxford, OX1 3PJ, UK

[3]Faculty of Engineering, Computing and Mathematics, University of Western Australia, Crawley, WA 6009, Australia

Abstract

This paper presents analysis of steady flow passing through a porous body in 3D, representing a steady current passing through a space-frame offshore structure such as an offshore jacket or a compliant tower. A porous body is used as a proxy for a space-frame structure to model the effect of current blockage, which may be interpreted as a global flow and force reduction relative to the standard Morison drag formulation due to the presence of the structure as a distributed obstacle. Both uniform and sheared approach flows are simulated with CFD in OpenFOAM for a porous body with uniformly distributed resistance. The behaviour of the blockage due to both types of flow are compared and contrasted using flow visualisation to illustrate the interaction of the flow with the body and the evolution of the resultant wake downstream of the body. The numerical results are compared with the actuator disc model for uniform flow due to [8] and the actuator disc model for sheared flow due to [1]. A porous body with non-uniform vertically distributed resistance is also considered, and the difference in the flow interaction relative to body with uniform resistance is analysed and discussed. The analysis provides the framework for applications for wind loading on offshore structures such as a space-frame during load-out and transportation on a barge, as well as numerical comparisons for an extension of the [1] model to an actuator disc with non-uniform resistance.

Introduction

When a steady current encounters a space-frame offshore structure such as jacket or compliant tower, on individual flow scales the current is flowing around each cylindrical member of the structure, but on a large scale there is a global flow divergence around the entire structure with the mean wake downstream. Because of the flow divergence, there is a reduction in the global flow velocity and associated hydrodynamic drag force relative to the standard Morison drag formulation, and this is interpreted as current blockage. Recently over a number of years, there have been extensive studies looking at the effect of blockage due to current as well as regular waves with in-line current, see e.g. [9, 7, 5, 6, 4]. For a problem where the length scale of global mean wake scales as the frontal width of an actual structure, a porous body can be used as a proxy in numerical CFD modelling with comparable amount of resistance distributed across the volume of the body.

Here we investigate the flow interaction of a steady current flow through a porous body, and compare the analysis in terms of mean reduced current flow velocity and resultant drag force using analytical and numerical CFD modelling. We also present some discussions on flow visualisation obtained from the CFD simulations. We consider three preliminary problems, as shown in table 1, of uniform and sheared approach flow on a porous body with uniformly distributed resistance (case 1 and 2), as well as uniform approach flow on a porous body with varying

resistance (case 3). For case 3, we prescribe a vertical linearly-varying resistance with fluid depth, such that the resistance at the upper portion is higher than the lower portion, but with the same overall resistance as the porous body with uniform resistance. The magnitude of the uniform approach flow for case 1 and 3 is prescribed to give approximately the same overall drag force on the porous body as for case 2. The aim is to better understand the physics of flow interaction and the wake structure downstream of the body. The intended application is for blockage due to current loading on space-frame offshore structures, but may also have application to wind loading during load-out and transportation on a barge.

Case	Current profile (m/s) & Forchheimer resistance profile (m^{-1})
1	$u_c(z) = 0.31$
	$F(z) = 32$
2	$u_c(z) = 0.1088z^2 + 0.7747z + 0.4765$
	$F(z) = 32$
3	$u_c(z) = 0.31$
	$F(z) = 32[3(z+0.495)+0.25]$

Table 1: Summary of the three cases considered, all assuming $\rho = 1000$ kg/m^3 and the depth of the flow, h, is set at 0.5 m.

Analytical models and numerical methodology

Analytical model

Two analytical models based on actuator disc theory are used for comparison with the numerical simulation. Here we give a brief introduction on each of the models. The fundamental assumption is that the flow is steady, incompressible and inviscid. Another assumption is the upstream fluid approaching an actuator disc/strip undergoes lateral expansion (or lateral divergence) only, without any vertical flow interaction.

Case 1: Uniform approach flow with uniform resistance.
Following [8] and [9], the simple current blockage model (hereafter termed SCB) developed for uniform approach flow demonstrates that the blocked current, u_{cs}, can be expressed in terms of the free-stream current, u_c, as:

$$u_{cs} = u_c / \left(1 + \frac{C_d A}{4A_f}\right), \tag{1}$$

where u_c is the incoming free-stream current, u_{cs} is the effective shielded (reduced) current at a structure, C_d is the drag coefficient, A is the solid drag area and A_f is the frontal area of the structure. The above expression is obtained after associating the mean force across the disc according to actuator disc theory (based on conservation of momentum across the disc and conservation of energy upstream and downstream of the disc) with

the drag force written in Morison form [3]. From Equation 1, the drag force can be written as:

$$\text{Drag (SCB)} = \frac{1}{2}\rho C_d A u_{cs}^2 = \frac{1}{2}\rho C_d A u_c^2 / \left(1 + \frac{C_d A}{4 A_f}\right)^2, \quad (2)$$

where ρ is the fluid density. To obtain the drag force prediction for SCB, a stick model which comprises a series of vertically-stacked actuator discs is used to represent the structure, with each disc acting independently of each other assuming no vertical flow interaction between each adjacent disc.

Following [1] for a more refined current blockage model (hereafter termed RCB) utilising an actuator strip, we have the following general result for the drag force:

$$\text{Drag (RCB)} = \int_{A_f} \Delta p \, dA_f = \frac{1}{2}\rho \int_{A_f} k(z)[u_{cs}(z)]^2 dA_f, \quad (3)$$

where $k = C_d A / A_f$, z is the vertical coordinate and the integral is over the frontal area of the structure. The above expression is subsequently evaluated in terms of integral of control volume upstream of the strip bounded by streamlines, of which the upstream frontal area is $A_{f1} = l_1 \times h = l_1/l \times A_f$, where h is the fluid depth and $l_1 = l/(1 + k/4)$ with l the lateral width of the strip. u_{cs} is related to the upstream velocity, u_c, as in Equation 1.

Case 2: Sheared approach flow with uniform resistance.
In this case, only u_{cs} and u_c vary with fluid depth. Since the velocity is uniform in the lateral direction, simplifying Equation 3 gives the drag force for case 2 as:

$$\text{Drag (RCB)} = \frac{1}{2}\rho \frac{kl}{\left(1 + \frac{k}{4}\right)^2} \int_0^h [u_c(z)]^2 dz. \quad (4)$$

Case 3: Uniform approach flow with varying resistance.
In this case, only k varies with fluid depth. Equation 3 becomes:

$$\text{Drag (RCB)} = \frac{1}{2}\rho u_c^2 l \int_0^h \frac{k(z)}{\left[1 + \frac{k(z)}{4}\right]^2} dz. \quad (5)$$

It is worth mentioning that the RCB model is originally developed to assess the performance of marine current/tidal turbines in shear flow, but is equally applicable for current blockage in shear flow and reduces to the SCB form for uniform approach flow (case 1).

Numerical model

The numerical setup is similar to that reported by [6] and recently by [4], using the same porous block approach in OpenFOAM® (http://www.openfoam.com) and the numerical wave tank 'waves2Foam' developed by [2]. Two-phase problem is solved where the free-surface becomes the interface between water and air, and volume-of-fluid (VOF) transport equation is used to capture the surface. The local Morison stress formulation is embedded in a porous block with the resistance specified by the Forchheimer parameter (F). At the location of the porous body, the modified Navier-Stokes momentum equation with the additional stress formulation is used, everywhere else in the computational domain the standard Navier-Stokes momentum equation is solved.

Just as the empirical drag coefficient (C_d) is required for the predictions of steady current forces on the structure, it is necessary to prescribe the value of the Forchheimer resistance parameter in our porous body simulation. Following [5, 6], the following

relationship holds for the calibration of the Forchheimer resistance (F) parameter: $C_d A / A_f = FL$, where L is the downstream length of the porous body. Isotropic resistance is assumed in this study.

Both uniform and sheared current profile are generated in the numerical wave tank by specifying a steady horizontal velocity profile, which could vary with water depth, at both the inlet and outlet to ensure mass conservation in the tank. This numerical approximation inevitably induces some artificial internal circulation, hence the zone of interest including the location of the porous body has to be placed nearer to the inlet and at sufficiently far distance away from the outlet to ensure the flow solutions are not affected by the approximation. The current profile is initialised throughout the computational domain, and the simulation is run until the current interaction with the porous body reaches steady-state behaviour.

In this paper, we consider a 3D computational domain spanning from 0 m (inlet) to 12 m (outlet) in streamwise direction, with the porous body located at 3.2 m from the inlet. The width of the domain is 1.2 m, and the height is 1 m, with the water depth set at 0.5 m from a frictionless bed. The porous body is made of a square cross-section of 0.12 m × 0.12 m, and the height is 0.7 m (protruding out the water surface). Hence, $L = 0.12$ m, $A_f = 0.06$ m², and F is set to be 32 m⁻¹. In the computational domain, the x coordinate runs horizontally in the streamwise direction, the y coordinate runs horizontally in the spanwise direction and the z coordinate runs vertically (with +ve upwards). The numerical prediction of the drag force is obtained by depth integration of the disturbed flow kinematics in the wetted portion of the porous body in a similar manner as described in [6].

Results and discussions

Reduced flow and drag force

Figure 1 shows the evolution of the reduced streamwise flow profile obtained from CFD (solid lines) taken along $y = 0$ (centreline of the porous body) from the inlet to front, middle and rear faces of the porous body for case 1 (left), case 2 (middle) and case 3 (right). As expected, streamwise flow reduction is observed as the approached flow encounters the porous body. The wake structure downstream of the body is not shown but can be observed from the flow visualisation presented in the next subsection. Due to the lateral flow divergence inside the porous body, the reduced streamwise flow profile varies along the lateral width (y) of the porous body. For case 1, one can observe the flow reduction is quite uniform across the water depth, while for case 2 and 3, the reduction is non-uniform. Also shown are the analytical predictions (dashed lines) at the middle of the porous body. In general the agreement is good. Larger discrepancy for case 2 may be attributed to the vertical flow interaction which enhances the streamwise velocity component at the lower portion of the water depth, as visible from figure 2.

The predictions from the two analytical and CFD models are summarised in table 2 in terms of two bulk flow properties: mean u_{cs} and drag force. For all three cases, the agreement between the analytical and CFD models in terms of mean u_{cs} is good. There is more differences in the drag force, noting that the porous resistance in CFD is based on the full Morison drag form, i.e. in streamwise direction, the drag form is $1/2\rho A_f F L u_x \sqrt{u_x^2 + u_y^2 + u_z^2}$ integrated over the volume of the porous body. Hence, because there is no account of three dimensional flow field in the drag form of the analytical models, the CFD prediction is slightly higher. In general, the agreement between CFD, SCB and RCB predictions in terms of drag force

Case	Mean u_{cs} (m/s)		Drag (N)			Mean u_{cs} (m/s)	Drag (N)
	CFD	SCB/RCB	CFD	SCB	RCB	CFD without porous body	
1	0.155	0.158	3.13	2.88		0.310	11.04
2	0.150	0.147	3.10	2.88	2.82	0.292	11.04
3	0.168	0.169	3.00	2.70	2.68	0.310	10.89

Table 2: Summary of the predictions in terms of mean bulk flow properties.
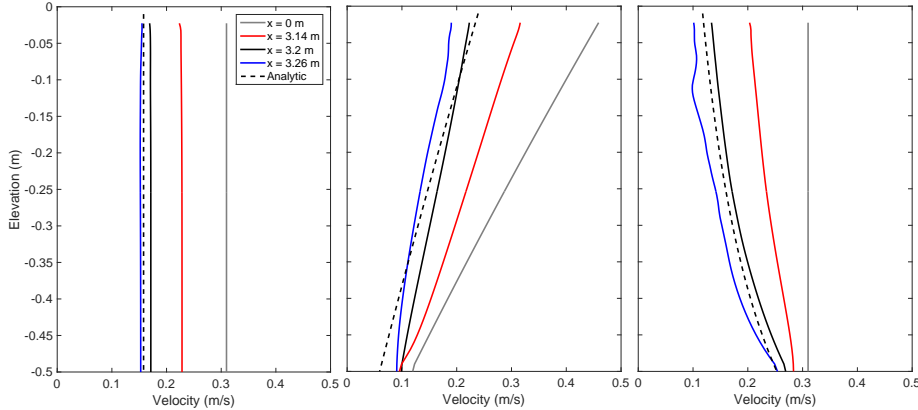
Figure 1: Evolution of the numerical sheared current profile (solid lines) with depth from the inlet to front ($x = 3.14$m), middle ($x = 3.2$m)and rear ($x = 3.26$m) faces of the porous body for case 1 (left), case 2 (middle) and case 3 (right) taken along $y = 0$ (centreline of the porous body). Also shown are the analytical predictions (dashed lines) at the middle of the porous body.

for all three cases is considered satisfactory. The good agreement indicates that the dominant flow interaction for all cases considered here is the lateral flow divergence, with smaller effect from the vertical flow interaction. Also shown is the predictions from the CFD without the presence of the porous body, which is equivalent to using standard Morison [3] formulation with no account for current blockage, to illustrate the amount of flow and force reduction due to different approach flows and different resistance loading.

Flow visualisation

Figure 2 presents flow visualisation all three cases. The details of the flow information is provided in the figure caption. All flow visualisation is taken when the flow has fully developed local to the structure; i.e. when the drag force reaches steady-state. The air phase is not shown. Because the flow visualisation is taken from a vertical slice, laterally diverging flow (with direction normal to the slice) is not obvious for the left panel. However, the existence of such diverging flow can be observed from the right panel.

In the top panels for case 1, because of the uniform loading exerted on porous body with uniformly distributed resistance, there is negligible vertical flow interaction; the flow reduction (blockage effect) is uniform over the water depth and the flow simply simply flows through or diverts laterally around the body (not visible in this vertical slice). Downstream of the body, the wake structure of the reduced flow is quite uniform with water depth, followed by some flow re-circulation and vertical flow interaction, before the reduced flow tends to recover towards the ambient flow at far downstream. Looking at the horizontal slice for uniform approach flow, one can see the lateral flow divergence around the body and the shear layers shed through the edges of the body. The width of the global wake behind the body is observed to be quite constant before slowly narrowing far downstream. The wake structure downstream of the body is relatively simple for uniform approach flow.

In the middle panels for case 2, however, the non-uniform loading exerted on the same porous body induces higher resistance (blockage) in the upper portion of the water column than in the lower portion, which causes the tendency of the flow to go downwards, as indicated by the black arrows in the vertical slice. Because of the higher blockage, the upper flow immediately downstream of the body is reduced relatively more than the lower flow, and hence there is a strong tendency for the lower flow to flow back up the water column further downstream of the body. From the horizontal slice, one can see similar flow structure as that of case 1, but there is a more complex structure further downstream due to stronger vertical flow interaction. Such complex wake structure might have implications on the performance of arrays of marine current/tidal turbine subjected to sheared approach flow, although it should be noted that the simulations herein are for an inviscid flow and the wake is developing.

In the bottom panels for case 3, there is some vertical flow interaction within the porous body due to non-uniform resistance loading exerted on the fluid by the structure. More reduction at the upper portion of the flow is observed because of the higher resistance than the lower portion, but most of the flow simply flows through the tower horizontally as well as laterally (again not visible in this vertical slice). Downstream of the body, there is a tendency for the lower flow to flow back up the water column similar to case 2. From the horizontal slice, the global mean wake structure downstream of the body is similar to that of case 1, which is relatively simple. We observe that the more skewed the resistance distribution is, the stronger the resultant vertical flow interaction.

Similar flow behaviour is also observed for horizontal and vertical slices taken at different locations, confirming the general trends of the flow behaviour.

Conclusions

Three different cases of approach flow interacting with a porous
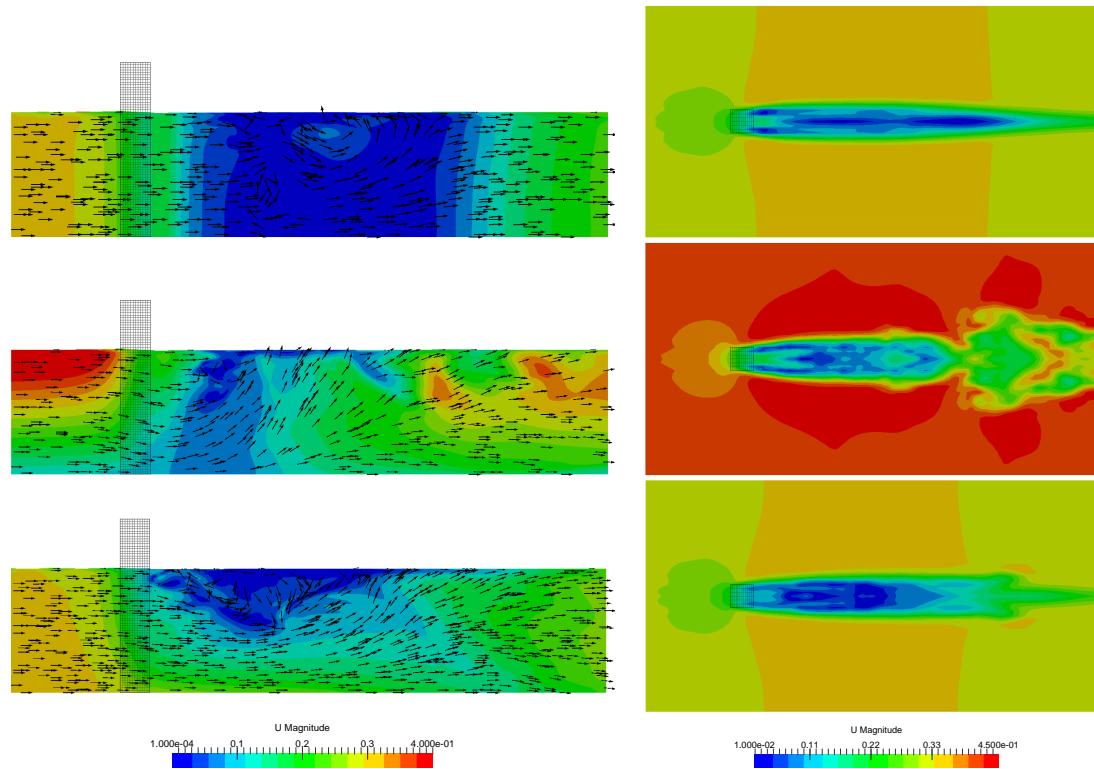
Figure 2: Flow visualisation of case 1 (top), case 2 (middle) and case 3 (bottom) for an approach flow through a porous body taken within the central portion of the computational domain. The porous body location is indicated by a block of black coloured mesh, while the flow is coloured based on the magnitude of the velocity. Left panel: Side view of the flow structure taken from a vertical slice along $y = 0$ m. The component of the flow velocity vector in the visualisation plane is shown as a black arrow on the figure. Right panel: Plan view of the flow structure taken from a horizontal slice at $z = -0.1$ m, where $z = 0$ corresponds to mean water level.

body having uniform and non-uniform resistance have been simulated in CFD and compared with the analytical predictions. In general, the bulk flow properties in terms of mean reduced streamwise flow velocity and drag force between the CFD and the two analytical predictions agree reasonably well. In particular, the RCB model captures the same trends in agreement with CFD, i.e. less drag force for case 2 and 3, all relative to case 1. Some indication of vertical flow interaction is observed from the reduced streamwise flow profile, which is supported by the observations from flow visualisation. We find that for case 1, the vertical flow interaction is negligible, the flow reduction is uniform over the water depth, and hence the resultant wake structure downstream is relatively simple. For case 2 and 3 however, the reduction is non-uniform over the water depth, and there is stronger vertical flow interaction occurring inside and downstream the porous body, which is consistent with small differences between the analytical predictions and CFD simulations of the velocity profile within the body. The wake structure downstream of the body is more complex, which might have implications on the performance of arrays of marine turbines subjected to sheared approach flow.

References

[1] Draper, S., Nishino, T., Adcock, T., Taylor, P., Performance of an ideal turbine in an inviscid shear flow. *Journal of Fluid Mechanics* **796**, 2016, 86–112.

[2] Jacobsen, N. G., Fuhrman, D. R., Fredsøe, J., A wave generation toolbox for the open-source CFD library: OpenFOAM®. *International Journal for Numerical Methods in Fluids* **70 (9)**, 2012, 1073–1088.

[3] Morison, J., O'Brien, M., Johnson, J., Schaaf, S., The force exerted by surface waves on piles. *Journal of Petroleum Technology* **2 (5)**, 1950, 149–154.

[4] Santo, H., Stagonas, D., Buldakov, E., Taylor, P. H., Current blockage in sheared flow: Experiments and numerical modelling of regular waves and strongly sheared current through a space-frame structure. *Journal of Fluids and Structures (under review)*, 2016.

[5] Santo, H., Taylor, P. H., Bai, W., Choo, Y. S., Blockage effects in wave and current: 2D planar simulations of combined regular oscillations and steady flow through porous blocks. *Ocean Engineering* **88**, 2014, 174–186.

[6] Santo, H., Taylor, P. H., Bai, W., Choo, Y. S., Current blockage in a numerical wave tank: 3D simulations of regular waves and current through a porous tower. *Computers & Fluids* **115**, 2015, 256–269.

[7] Santo, H., Taylor, P. H., Williamson, C. H. K., Choo, Y. S., Current blockage experiments: force time histories on obstacle arrays in combined steady and oscillatory motion. *Journal of Fluid Mechanics* **739**, 2014, 143–178.

[8] Taylor, P. H., Current blockage: reduced forces on offshore space-frame structures. *In: Offshore Technology Conference*, OTC 6519, 1991.

[9] Taylor, P. H., Santo, H., Choo, Y. S., Current blockage: reduced Morison forces on space frame structures with high hydrodynamic area, and in regular waves and current. *Ocean Engineering* **57**, 2013, 11–24.